

Faceting transition in epitaxial growth of dilute GaNAs films on GaAs

M. Adamcyk,^{a)} S. Tixier, B. J. Ruck, J. H. Schmid, and T. Tiedje^{b)}

Department of Physics and Astronomy, University of British Columbia, Vancouver, BC, V6T 1Z1 Canada

V. Fink, M. Jeffries, D. Karaiskaj, K. L. Kavanagh, and M. Thewalt

Department of Physics, Simon Fraser University, Burnaby, BC, V5A 1S6 Canada

(Received 28 December 2000; accepted 26 May 2001)

An abrupt transition to a {111} faceted growth mode is observed in molecular-beam-epitaxy growth of dilute $\text{GaN}_x\text{As}_{1-x}$ ($x < 0.05$) films on (100) GaAs substrates. The faceted growth mode is favored by high growth temperatures, high nitrogen content, and high arsenic flux. The best electronic quality material, as measured by low-temperature photoluminescence, was obtained at high growth temperatures and high arsenic flux without exceeding the threshold for facet formation. The nitrogen content was found to be insensitive to the arsenic flux. © 2001 American Vacuum Society. [DOI: 10.1116/1.1386379]

I. INTRODUCTION

Recently, much progress has been made on improving the material quality of $\text{GaN}_x\text{As}_{1-x}$ and $\text{In}_y\text{Ga}_{1-y}\text{N}_x\text{As}_{1-x}$ semiconductor thin films grown by solid-source molecular-beam epitaxy (MBE). The incorporation of dilute ($x < 0.05$) amounts of nitrogen into GaAs results in an anomalous decrease of the band gap due to band-gap bowing. The addition of In to GaNAs reduces the tensile strain in the material caused by the small nitrogen atoms and further decreases the alloy's band gap, thereby yielding material that can exhibit optical emission in the technologically important 1.3–1.55- μm -wavelength range. Recently, there has been considerable interest in using the dilute nitrides as the active material in semiconductor lasers grown on GaAs substrates.^{1,2}

The GaNAs alloy system has a wide miscibility gap due to the large difference in size of N and As atoms. As a result, nonequilibrium growth techniques such as MBE must be used in order to grow single-phase crystals with high nitrogen concentrations. Phase separation has been observed in concentrated $\text{GaN}_x\text{As}_{1-x}$ ($x = 0.2$) grown by MBE on GaP.³ However, it has been shown that by pushing the growth process further out of equilibrium (by decreasing the substrate temperature, for example), phase separation can be avoided.⁴

In this article, we study the growth of GaNAs by solid-source MBE. We find that growth conditions which favor adatom surface diffusion (higher substrate temperature, higher As_2 flux, and low growth rate) lead to rough surfaces and three-dimensional (3D) growth. In particular, while keeping all other growth parameters constant, we show that a variation of the arsenic overpressure can cause a transition from a smooth two-dimensional (2D) growth to a faceted three-dimensional growth. To our knowledge, this is a new morphological transition not previously reported in strained GaNAs films. The thin films are characterized using real-time elastic light scattering, transmission electron micro-

scopy (TEM), scanning electron microscopy (SEM), photoluminescence (PL), and high-resolution x-ray diffraction (XRD).

II. EXPERIMENT

The GaNAs heteroepitaxial growth experiments were carried out in a VG-V80H MBE deposition system, equipped with a conventional Knudsen effusion cell for Ga and a two-zone cracker source for As_2 . Active nitrogen was produced by a novel helical resonator rf plasma source equipped with a pyrolytic boron-nitride baffle for the elimination of ions and energetic neutrals. Ultrahigh-purity nitrogen is introduced into the plasma source using a leak valve. The downstream side of the leak valve is differentially pumped by a throttled turbopump in order to regulate the pressure in the discharge and to maintain a gas flow. Flowing gas through the source minimizes the effect of impurities produced by outgassing in the gas inlet system. The substrate temperature was monitored throughout the growth using an optical band-gap thermometer with an absolute accuracy of about $\pm 2.5^\circ\text{C}$. Prior to loading into the MBE system, polished (100)-oriented, on-axis ($\pm 0.5^\circ$), GaAs substrates were oxidized by exposure to UV ozone. This process reduces carbon contamination on the substrate surface. After the samples were loaded into the growth chamber, the substrate was ramped up in temperature to 615°C under an As_2 overpressure for approximately 20 min to remove the native surface oxide.

Unless otherwise specified, the growth rate was 10.4 nm/min, as determined by *ex situ* x-ray diffraction measurements. The beam-equivalent pressure (BEP) was measured with a retractable ion gauge and the V/III ratio varied from 6 to 18 depending on the arsenic flux. All growths were carried out on the As-terminated 2×4 surface reconstruction of GaAs. Following the growth of a 200-nm-undoped GaAs buffer layer, GaNAs growth was initiated by igniting a plasma in the nitrogen source. The net rf power transmitted to the source (forward minus reflected) was 70 W at a frequency of 200 MHz. We controlled the nitrogen content of the film, at fixed substrate temperature, by varying the nitrogen pressure in the discharge. During the GaNAs

^{a)}Electronic mail: adamcyk@physics.ubc.ca

^{b)}Also at: Department of Electrical and Computer Engineering, University of British Columbia, Vancouver, BC, V6T 1Z1 Canada.

growth, the background nitrogen pressure in the growth chamber ranged from 1.5 to 7.0×10^{-6} mBar depending on the target nitrogen content.

X-ray diffraction experiments as a function of As_2 indicate that the magnitude of the As_2 flux only weakly affects the nitrogen incorporation in the films. Midway through the growth of a 0.9% GaNAs film, the As_2 flux was decreased by 40%. A high-resolution x-ray rocking curve taken on this sample showed no detectable broadening of the diffraction peak for the epilayer, consistent with a less than about 5% change in the nitrogen content. From a practical perspective, this greatly simplifies the growth of these materials as this means that the nitrogen content can be controlled independently without precise control over the As_2 flux. In these experiments, the GaNAs films were typically grown to a thickness of 300 nm. The GaNAs growth was stopped by closing the Ga shutter and turning off the plasma simultaneously, after which the substrate heater was shut off to quench the sample by radiative cooling to the liquid-nitrogen-filled cryoshroud. The cooling rate was approximately $60^\circ\text{C}/\text{min}$ at the growth temperature, but dropped to about $20^\circ\text{C}/\text{min}$ below 300°C .

The surface morphology of the films was monitored during growth using elastic light scattering with 254-nm-wavelength light from a 100 W Hg arc lamp. The light-scattering experiment is described in more detail in a previous publication.⁵ The power spectral density (PSD) of a surface is defined as the Fourier transform of the surface height-height autocorrelation function. The light-scattering signal is proportional to the PSD of the surface roughness at a spatial frequency q defined by the scattering geometry and the wavelength of the incident light. The scattered light was detected at a backscattering angle so as to maximize the in-plane spatial frequency to which the measurement is sensitive. For our scattering geometry, the scattered light depends on surface roughness with a spatial frequency of $41 \mu\text{m}^{-1}$, or equivalently, to a length scale of 154 nm, during film growth.

III. RESULTS AND DISCUSSION

The inset in Fig. 1 shows typical light-scattering data taken during the thermal oxide desorption process, the subsequent surface annealing in an As_2 flux, and during the beginning of the growth of a GaAs buffer layer. The time axis is shifted so that $t=0$ corresponds to the start time of the anneal. Immediately after the initial roughening caused by the explosive oxide desorption, the surface smoothes, approaching a steady-state roughness after 10 or 15 min. The surface smoothing during the As_2 anneal is shown in the main panel of Fig. 1 for two different As_2 overpressures and the same substrate temperature. Here, the extrapolated background corresponding to the steady-state roughness has been subtracted from the data (see, for example, the line marked "A" in the inset of Fig. 1). The data in Fig. 1 show that the surface smoothing rate increases by a factor of 2 with a threefold increase in As_2 pressure. We interpret this result to mean that the Ga diffusion on the surface increases with the As_2 overpressure. Atomic-force microscopy images (not

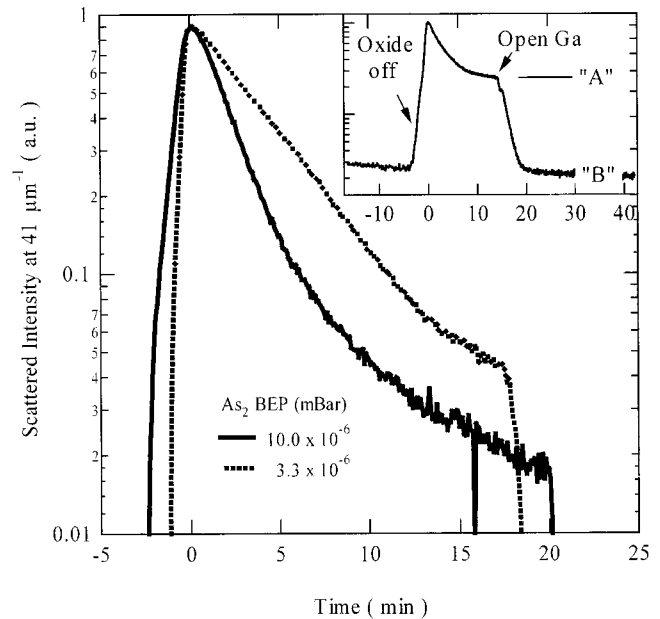


FIG. 1. Light-scattering signal measured at a spatial frequency of $41 \mu\text{m}^{-1}$ during thermal oxide desorption from a GaAs substrate prior to MBE growth. The substrate temperature was held at 615°C for $t > 0$. The background signal coming from the steady-state roughness of the oxide desorbed surface (marked "A" in the inset) has been subtracted from the data. The inset shows the scattered light intensity as a function of time during the oxide desorption, anneal, and subsequent buffer layer growth, with no background subtraction.

shown) from GaAs homoepitaxial samples grown under similar conditions with different As_2 overpressures, show that a high group-V flux decreases the anisotropy in the surface structure and decreases the surface roughness. We conclude that the anisotropy decreases and the magnitude of the surface diffusion increases with increasing As_2 pressure. These results are consistent with the work of LaBella *et al.*⁶ who, using a combination of MBE and scanning tunneling microscopy, observed a similar increase in Ga surface diffusion on GaAs with increasing As_4 overpressure. Additionally, our findings agree with the work of Pinnington,⁷ who showed that indium diffusion on GaAs increased with As_2 overpressure.

We now focus our attention on two GaNAs growths carried out at different As_2 overpressures, at a substrate temperature of 500°C . We label the sample grown at high As_2 pressure ($\text{BEP} = 10.0 \times 10^{-6}$ mBar) as H and the sample grown at low As_2 pressure ($\text{BEP} = 3.3 \times 10^{-6}$ mBar) as L. Samples H and L were 40 and 350 nm thick, respectively. In both films, the nitrogen content expressed as a fraction of the group-V atoms was found to be 1.8%. The nitrogen content was determined from high-resolution XRD calibrated by secondary ion mass spectroscopy (SIMS) measurements on test samples. Figure 2 compares the light-scattering signal measured at $41 \mu\text{m}^{-1}$ during the growth of samples H and L. The time axis is shifted so that $t=0$ corresponds to the time at which the plasma is ignited, or in other words, the start of the nitrogen alloy deposition. The inset in Fig. 2 shows the light-scattering data for the sample that roughens (H). The back-

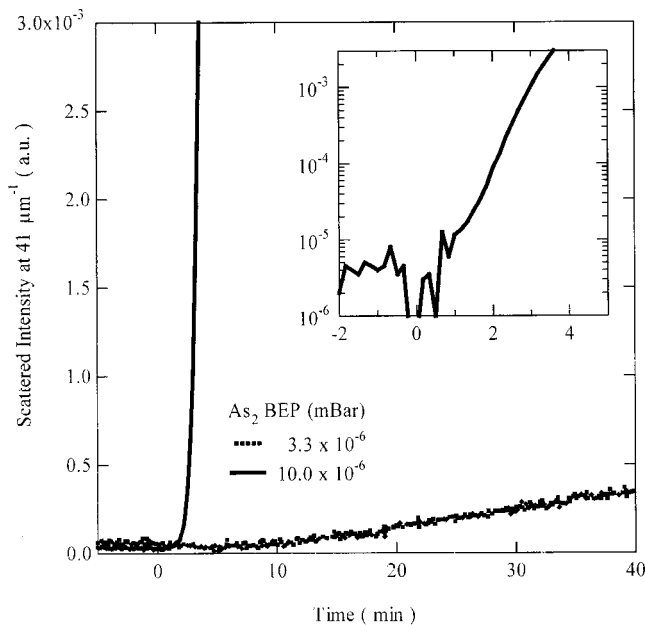


FIG. 2. Light scattering measured at a spatial frequency of $41 \mu\text{m}^{-1}$ during the growth of 1.8% GaNAs for two different runs carried out at a substrate temperature of 500°C but with different As_2 overpressures. The inset shows the data taken from the sample grown with a high As_2 flux with the background scattering from the buffer layer subtracted from the data.

ground scattering from the GaAs buffer layer was subtracted from the data in order to distinguish the scattering associated with the growth of the GaNAs layer. As an example, the background signal from the buffer is indicated by the line marked “B” in the inset of Fig. 1. The inset in Fig. 2 shows that sample H, which was grown at high arsenic flux, began to roughen immediately after the ignition of the plasma. The sample grown at low arsenic flux (L) showed no significant roughening and the sample surface retained a mirror-like appearance.

A SEM image taken from a nominally 300-nm-thick GaNAs film grown under the same conditions as sample H is shown in Fig. 3(a). The surface of the crystal is rough and has pyramid-shaped pits whose depth is on the order of the

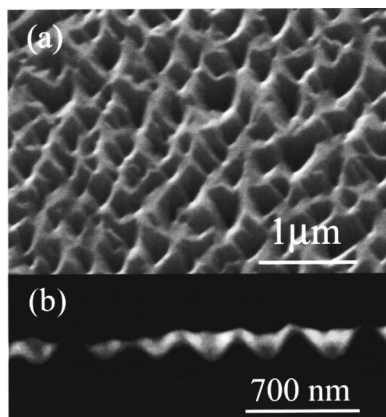


FIG. 3. Scanning electron microscope image of a rough, three-dimensional GaNAs film grown on GaAs viewed at an angle of approximately (a) 45° and (b) 90° with respect to the sample normal.

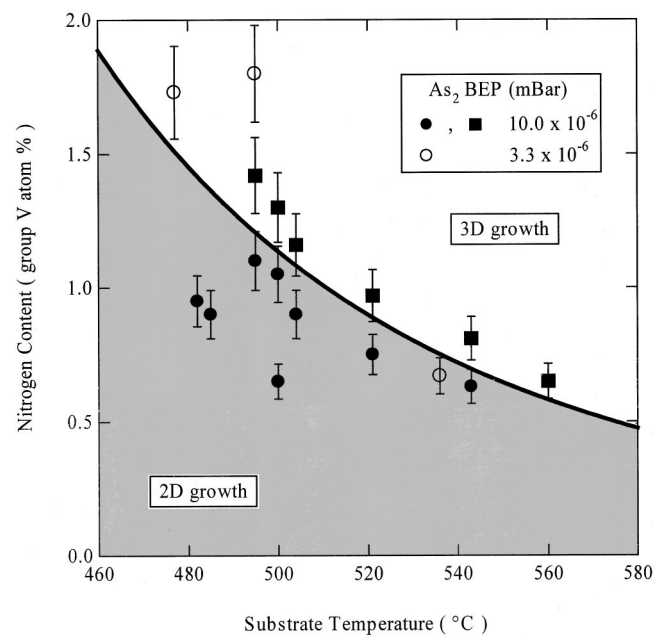


FIG. 4. Phase diagram showing the boundary between smooth and faceted GaNAs films on GaAs. The position of each marker indicates the composition and growth temperature of the GaNAs epilayer. The films indicated by square and round markers are faceted and smooth, respectively.

film thickness, which suggests 3D growth. Figure 3(b) gives a cross-section view of the sample and shows that the sidewalls of the pits are smooth. Analyzing several images similar to Fig. 3(b) taken from the same sample, we found that the sloped sidewalls make an average angle of 52° with the $[100]$ crystal direction. This is consistent with the formation of $\{111\}$ facets during the growth for which we would expect facets oriented at 54° with respect to $[100]$. The transition from 2D to 3D growth is also observed as a function of nitrogen content and growth temperature. High growth temperatures and high nitrogen contents favor 3D growth. Figure 4 maps out the growth temperature and nitrogen content at which the faceting transition occurs. Growth runs carried out under two different As_2 overpressures are shown, with an As_2 beam-equivalent pressure of 3.3×10^{-6} and 10.0×10^{-6} mBar. The square symbols indicate samples that exhibited 3D growth and the circular symbols indicate 2D growth.

The solid line in Fig. 4 is a fit of an Arrhenius function to the border between the smooth and faceted films for the high As_2 overpressure growth conditions. The fitted curve has an activation energy of 0.62 eV. Given that the 3D growth mode is favored by high nitrogen content, high arsenic flux (which increases surface diffusion), and high growth temperature, it is tempting to interpret the rough growth mode as a sign of GaN/GaAs phase separation. One would expect phase separation to be favored by the parameters mentioned above that enhance the surface roughening. However, x-ray diffraction, transmission electron microscopy, and Raman scattering measurements failed to detect any GaN phase in the GaNAs films. We, therefore, propose an alternate explanation, namely, that the nitrogen incorporation affects the

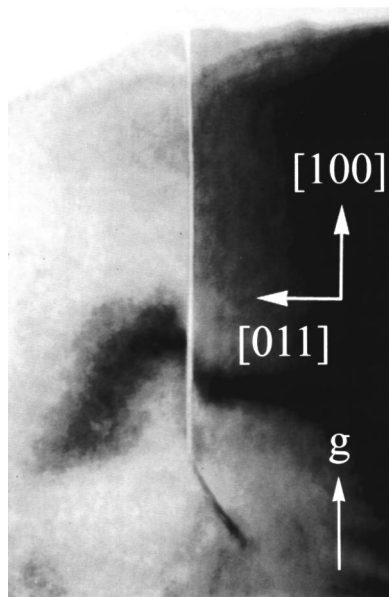


FIG. 5. Bright-field transmission electron microscopy image, $g=(400)$, taken from a $\{011\}$ cross section of a 2.2% GaNAs/GaAs film. A crack is seen to propagate from the surface through the interface into the substrate. No misfit dislocations are visible in the sample. The change in direction of the crack inside the substrate near the crack tip is consistent with a change in fracture surface from $\{011\}$ to $\{111\}$ planes. The surface roughness amplitude is about 5 nm.

surface energy and lowers the relative energy of the $\{111\}$ facets with respect to the $\{100\}$ surface, thereby favoring the formation of $\{111\}$ facets. The onset of faceting has the form of a phase transition with an abrupt transition to a rough surface at a critical value of the nitrogen content. All of the samples grown at low As_2 overpressure had a mirror-like surface morphology. This suggests that the threshold for faceting under these growth conditions occurs at higher nitrogen content than was studied here.

Dark-field optical microscopy results show that although sample L is smooth, cracks are present on the surface. These cracks are aligned parallel to the $[01\bar{1}]$ crystal direction and are approximately $10\ \mu\text{m}$ apart. No cracks were observed in the orthogonal $[110]$ direction. A (400) bright-field TEM image of a crack observed in cross section from a 340-nm-thick 2.2% GaNAs film is shown in Fig. 5. Assuming Vegard's law, the misfit strain in the sample was 0.45%. This sample was grown under the same conditions as low arsenic flux sample L, except for a slightly higher nitrogen flux. The interface between the GaNAs layer and the GaAs buffer layer is not visible in the TEM image in Fig. 5. Although clear pendellosung fringes are visible in x-ray diffraction on strained samples, they were not present in scans taken from strain-relaxed samples, presumably because of the elastic distortion associated with the cracks. Therefore, we could not directly measure the thickness of the cracked sample using x rays. However, based on the nominal growth rate of the sample determined by x-ray diffraction on calibration runs, we conclude that the cracks penetrate through the interface with the substrate. The change in direction of the crack in the

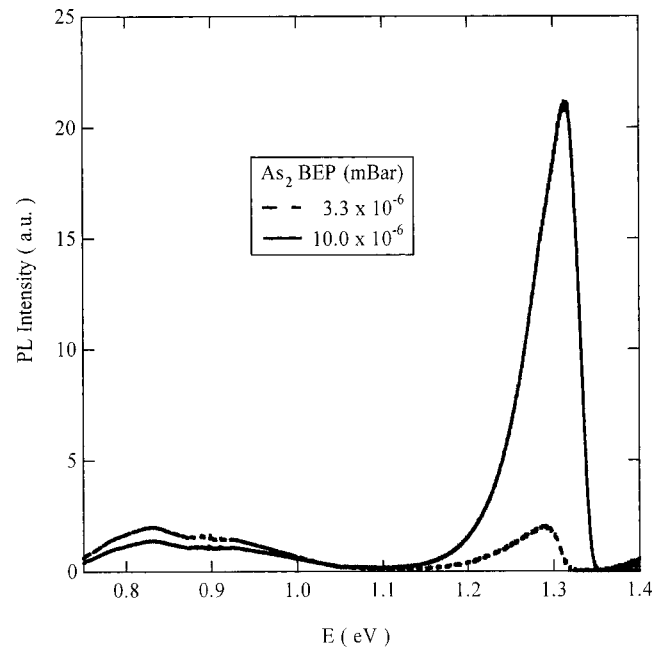


FIG. 6. 4.2 K photoluminescence taken from two nominally 0.7% GaNAs samples grown at a substrate temperature of 540 °C under different As_2 overpressures.

substrate is consistent with the crack switching to a $\{111\}$ plane from a $\{011\}$ plane. A similar change in crack propagation direction has been observed in tensile-strained InGaAs/InP by Wu and Weatherley.⁸ These authors point out that the strain parallel to the crack in the substrate favors a change in direction of propagation of the crack. Since misfit dislocations are not observed in our tensile-strained films, we presume that the threshold for crack formation occurs before the threshold for formation of misfit dislocations.

Similar cracks have been observed in tensile-strained GaNP/GaP,⁹ InGaAs/InP,⁸ and AlGaIn/GaN¹⁰ films. In the 2% tensile-strained InGaAs/InP system, cracks form along the $[011]$ direction rather than along $[01\bar{1}]$, as in our samples. Hearne *et al.* have observed crack formation during the growth of AlGaIn/GaN heterostructures having tensile strain in the 0.5% range,¹⁰ which is similar to the strain in our 2.2% GaNAs sample. The authors also found that crack formation occurs before the nucleation of misfit dislocations. Our experiments do not permit us to determine if the cracks occurred during growth or during sample cooling. The absence of changes in the surface profile due to deposited material around the open end of the crack shown in Fig. 5 suggests that the cracks form during the cool down. Because of the relatively large spacing between the cracks ($\sim 10\ \mu\text{m}$), the light-scattering measurement, which is sensitive to length scales of 154 nm, does not detect the crack formation.

The photoluminescence was found to be sensitive to the As_2 overpressure during the growth. In Fig. 6 we show low-temperature PL spectra for two nominally 0.7% GaNAs films grown at 540 °C with different As_2 pressures during growth. Although the As_2 overpressures were different during these two growths, both films were grown in the smooth two-

dimensional regime. The intensity of the defect luminescence in the far-infrared region of the spectrum is similar for both samples. However, the band-to-band luminescence is ten times stronger for the film grown at higher As₂ overpressure. The full width at half maximum of the band-to-band luminescence is about 62 meV for both samples. Samples grown at lower substrate temperatures (480–500 °C) under high As₂ overpressure did not produce such intense band-to-band photoluminescence, thereby indicating that the combination of a higher growth temperature and higher As₂ flux improves the electronic quality of the material. Further improvements in PL emission are possible with rapid thermal annealing.

IV. CONCLUSION

Experiments on MBE growth of dilute alloy films of strained GaN_xAs_{1-x} on GaAs show that the surface morphology and photoluminescence are sensitive to the As₂ flux while the N content is not sensitive to the flux. At a threshold value of the As₂ overpressure that depends on growth temperature and nitrogen flux, the GaNAs surface forms {111} facets, with high arsenic flux favoring faceting. We attribute the faceting to a lowering of the relative energy of {111}

surfaces with respect to the (100) surface caused by nitrogen incorporation. High arsenic flux also leads to improved photoluminescence efficiency.

ACKNOWLEDGMENTS

The authors are grateful to R. Streater for the SIMS analysis, W. Hardy for help with the nitrogen source, and J. Trodahl for the Raman scattering measurements.

- ¹M. Fischer, M. Reinhardt, and A. Forchel, *Electron. Lett.* **36**, 1208 (2000).
- ²T. Kitatani, K. Nakahara, M. Kondow, K. Uomi, and T. Tanaka, *Jpn. J. Appl. Phys., Part 2* **39**, L86 (2000).
- ³J. W. Orton, D. E. Lacklison, N. Baba-Ali, C. T. Foxon, T. S. Cheng, S. V. Novikov, D. F. C. Johnston, S. E. Hooper, L. C. Jenkins, L. J. Challis, and T. L. Tansley, *J. Electron. Mater.* **24**, 263 (1994).
- ⁴W. G. Bi and C. W. Tu, *Appl. Phys. Lett.* **70**, 1608 (1997).
- ⁵T. Pinnington, Y. Levy, J. A. Mackenzie, and T. Tiedje, *Phys. Rev. B* **60**, 15901 (1999).
- ⁶V. P. LaBella, D. W. Bullock, Z. Ding, C. Emery, W. G. Harter, and P. M. Thibado, *J. Vac. Sci. Technol. A* **18**, 1526 (2000).
- ⁷T. Pinnington, Ph.D. thesis, University of British Columbia (1999).
- ⁸X. Wu and G. C. Weatherly, *Acta Mater.* **47**, 3383 (1999).
- ⁹N. Y. Li, W. S. Wong, D. H. Tomich, K. L. Kavanagh, and C. W. Tu, *J. Vac. Sci. Technol. B* **14**, 2952 (1996).
- ¹⁰S. J. Hearne, J. Han, S. R. Lee, J. A. Floro, D. M. Follstaedt, E. Chason, and I. S. T. Tsong, *Appl. Phys. Lett.* **76**, 1534 (2000).